Optical coherence tomography of the human skin

Julia Welzel, MD,[a] Eva Lankenau, MSc,[b] Reginald Birngruber, PhD,[b] and Ralf Engelhardt, MSc[b] *Lübeck, Germany*

Background: Optical coherence tomography (OCT) is a new diagnostic method for tissue characterization.
Objective: We investigated normal and pathologic structures in human skin in several locations to evaluate the potential application of this technique to dermatology.
Methods: Based on the principle of low-coherence interferometry, cross-sectional images of the human skin can be obtained in vivo with a high spatial resolution of about 15 μm. Within a penetration depth of 0.5 to 1.5 mm, structures of the stratum corneum, the living epidermis, and the papillary dermis can be distinguished.
Results: Different layers could be detected that were differentiated by induction of experimental blisters and by comparison with corresponding histologic sections. Furthermore, OCT images of several skin diseases and tumors were obtained.
Conclusion: OCT is a promising new imaging method for visualization of morphologic changes of superficial layers of the human skin. It may be useful for noninvasive diagnosis of bullous skin diseases, skin tumors, and in vivo investigation of pharmacologic effects.
(J Am Acad Dermatol 1997;37:958-63.)

Several imaging methods have been created to investigate morphologic changes in the skin. Epiluminescence microscopy and high-frequency ultrasound[1] are already established as diagnostic procedures. In combination with experimental methods such as confocal microscopy[2] and magnetic resonance tomography[3] it is possible to obtain information about skin surface morphology and dermal changes.

Optical coherence tomography (OCT) was introduced as a method for noninvasive investigation of the human eye.[4-9] Several studies have demonstrated that this technique can be used for visualization of low-scattering tissues like the cornea, lens, and retina. We created an OCT system for measuring the human skin.[10-16] The technique and its potential use in dermatology are described.

From the Department of Dermatology, Medical University of Lübeck,[a] and the Medical Laser Center, Lübeck.[b]
Supported in part by the German Ministry of Science and Research (BMBF), FK No. 13N6302.

MATERIAL AND METHODS

Technique

The OCT system is based on the principle of Michelson interferometry using short coherence length light. Infrared light from a 830 nm superluminescence diode is coupled into an optical fiber interferometer. The optical path length distribution of the sample beam measured by the interference modulation of the axial OCT scan can be interpreted as the depth resolved reflection signal of the sample. Interference occurs only when the propagation distance of both beams match within the coherence length of the light source. The amplitude of the interference modulation is detected, digitalized by an analog digital converter (ADC), and converted to a logarithmic gray scale. The low coherence length (here about 15 μm) determines the depth resolution of the system. Lateral scanning of the axial OCT scans results in two-dimensional cross-sectional images. The high dynamic range of 100 dB allows the detection of ultra-weak light signals and therefore tomographic images of maximal detection depth. The images can be compared with B-mode high-frequency ultrasound images but represent optical and not acoustical inhomogeneities of the tissue. The system is described elsewhere in detail.[14,15]

Human subjects

Numerous male and female adult volunteers participated in the study. The study was approved by the

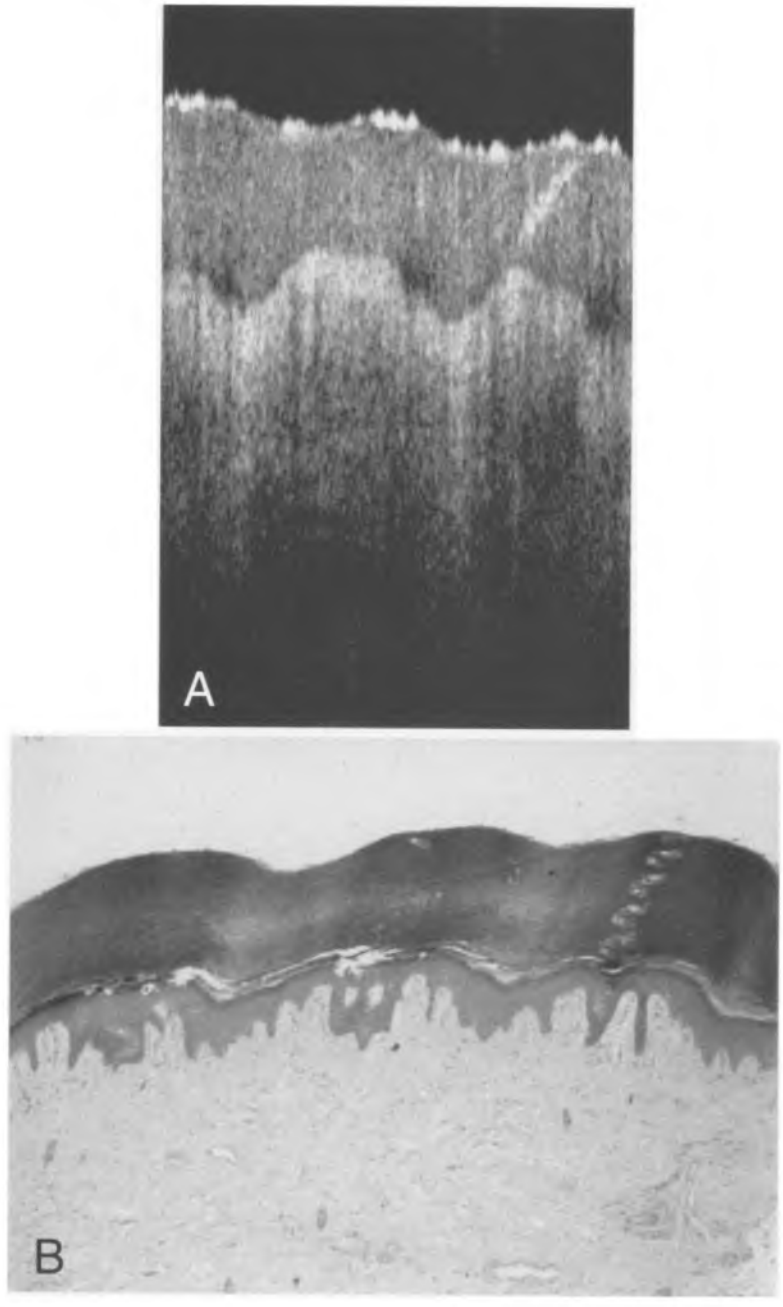

Fig. 1. Healthy skin of fingertip. **A,** OCT and **(B)** corresponding histology. The superficial layer is thick stratum corneum. Stratum lucidum is less dense. The signal dense deeper layer can be assigned to epidermis. Note sweat gland duct. OCT image: 1 × 1.5 mm. (**B,** Original magnification × 100.)

local ethics committee, and informed consent was obtained from each subject.

We investigated healthy skin at different locations as well as several skin diseases. The OCT images were compared with corresponding histologic sections. To distinguish between the different layers seen in OCT we induced blisters experimentally. Subepidermal blisters were produced with liquid nitrogen, and intraepidermal blisters were produced with mechanical stress. The cleft location was confirmed by biopsy.

Measurements

The volunteers were positioned comfortably in front of the system. On the test site the skin was pretreated with glycerol to reduce light reflection from the surface. The skin was positioned against an aperture of the

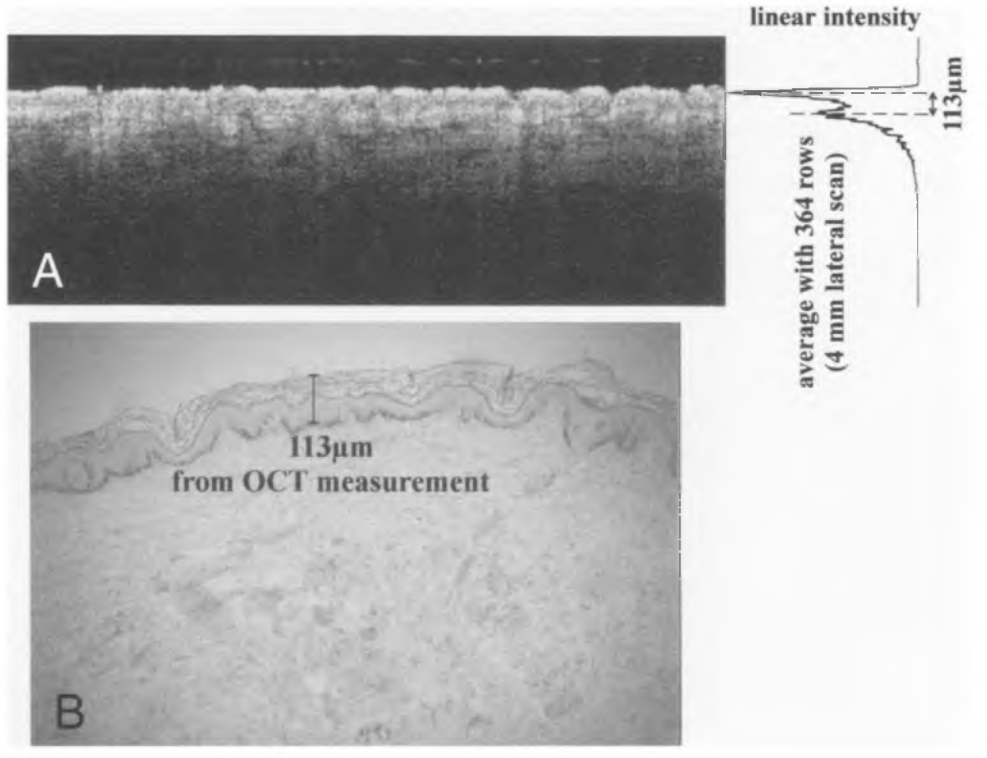

Fig. 2. Healthy skin of forearm. OCT (**A**) and corresponding histology (**B**). Superficial layer in OCT represents entire epidermis. Intensity peak below entrance signal corresponds to basement membrane zone. OCT image: 4 × 1.5 mm. (**B,** Original magnification × 100.)

measuring unit with mild pressure. The light beam was adjusted along the optical axis until the skin surface was brought into focus. The scan direction and length were selected depending on the size of the region of interest. The measurement was controlled by a video image of the sample beam location and movement. Simultaneously the OCT B-scan was displayed in real time on a screen. The measuring time for one image depended on the desired lateral resolution and scanning length. For a sample size of 4 mm and a lateral resolution of 10 µm, one OCT image took about 40 seconds. The measurement was performed without touching the skin surface.

The cross-sectional tomographs of the skin were represented in logarithmic false color or gray scale images. The axial dimension was corrected by the average refractive index of the skin of 1.4. This index was assumed to be approximately the same for normal skin in each location. The axial axis values were corrected by division by the index value.[17]

RESULTS

The correlation between OCT images and histology of normal skin can be seen in Fig. 1. The OCT cross sections showed differences depending on the location. On the palm, especially on the fingers, a thick stratum corneum could be distinguished. The lower layers were less signal intense and corresponded to the stratum lucidum. The living epidermis could be seen as a signal dense irregular layer with waves of papillary ridges. The papillary dermis appeared less dense. Spiral sweat gland ducts could be seen within the stratum corneum.

In forearm skin the stratum corneum was thinner (Fig. 2). The first layer seen in OCT represented the whole epidermis as confirmed by histology. The distribution of the intensities of the signal showed a slight peak below the entrance signal. The depth of this peak corresponded to the basement membrane zone.

A nail plate of the lunula region was demonstrated in OCT as a signal dense structure composed of parallel layers. The cuticle and the proximal nailfold could be distinguished from the matrix. The skin was transparent enough to allow a penetration of the signal even to the matrix region.

A subepidermal blister on the forearm caused by liquid nitrogen could be detected in OCT. The

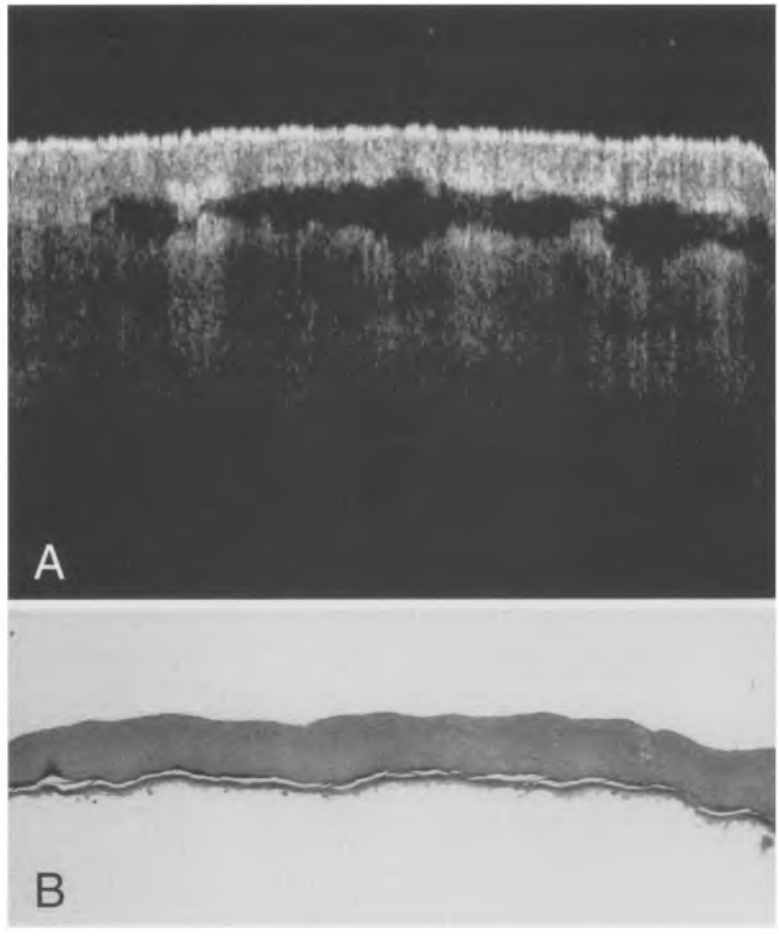

Fig. 3. Intraepidermal blister on thumb. **A,** Cleft location is below stratum corneum in OCT. **B,** Histology of roof of blister confirms that it contains only stratum corneum and stratum granulosum. OCT image: 2 × 1.5 mm. (**B,** Original magnification × 100.)

entire epidermis was elevated. The blister appeared as a dark area.

A mechanically induced blister on the thumb (Fig. 3) showed a cleft below the thick stratum corneum. The histology of the roof of the blister confirmed that the cleft started in the upper stratum spinosum. The roof consisted of the stratum corneum and the stratum granulosum. After the roof was removed, highly reflecting structures remained on the bottom of the blister corresponding to the lower epidermis.

A lentigo maligna melanoma is shown in Fig. 4. In the OCT image irregular structures could be detected in the lower epidermis that corresponded to the tumor cell aggregates in the histologic section. The basement membrane zone that could be detected in healthy skin in the OCT image as a second parallel line was absent in the tumor. Consecutive measurements of the same region confirmed that these changes were reproducible and not an artifact from speckle noise.

Even a scabies mite could be visualized with its tunnel-like burrow in the stratum corneum (Fig. 5).

DISCUSSION

Superficial human skin can be visualized with high-resolution OCT. Different layers of healthy skin can be distinguished as well as bullous changes and skin tumors. In conjunction with histologic examination we were able to assign the structures seen in OCT to microscopic morphology. In different experimentally induced bullous changes of the skin we were able to distinguish between the layers seen in OCT images.

The axial resolution of 15 μm allowed detection of cell aggregates and layers in skin diseases and tumors. However, investigation of single cells

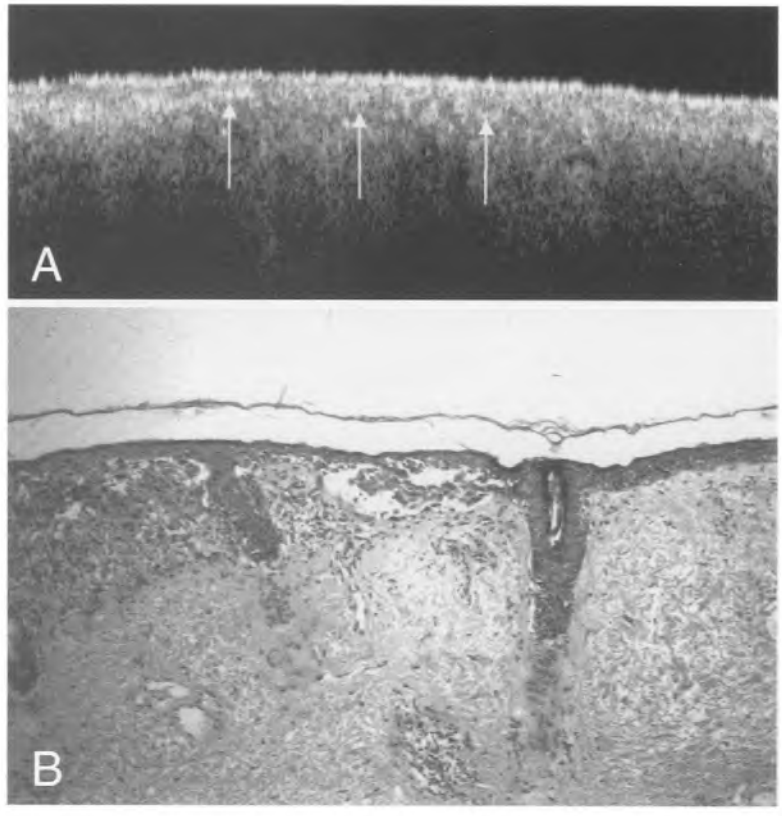

Fig. 4. OCT **(A)** and corresponding histology **(B)** of a lentigo maligna melanoma. On right side, note border to healthy skin. Melanoma nests on left side are represented as irregular structures in OCT *(white arrows).* OCT image: 2 × 0.8 mm. **(B,** Original magnification × 200.)

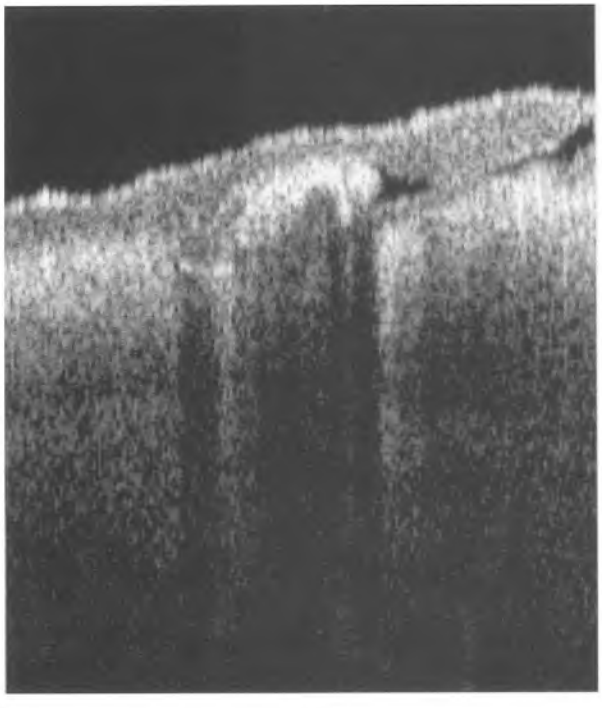

Fig. 5. OCT of scabies mite in center of image; burrow behind mite. 1 × 1.2 mm.

or subcellular structures was not possible. The detection depth of OCT is generally limited by multiple scattering and attenuation of the signal. The current detection depth of about 1 mm and the axial resolution of 15 μm were sufficient for investigation of the stratum corneum, the living epidermis, and upper parts of the dermis. Confocal microscopy has a higher resolution than OCT, but the detection depth is much lower. The lower resolution of high-frequency ultrasound leads to poor differentiation of epidermal structures. Thus OCT is an ideal intermediate between these two methods for investigation of the epidermis. Furthermore, it is simple, noninvasive, and rapid. The diagnostic potential of OCT may prove to be valuable in the detection of early stage melanoma or precancerous changes and the location of the cleft in bullous autoimmune diseases. OCT may also be helpful for investigation of steroid atrophy or wound healing.

REFERENCES

1. Altmeyer P, el-Gammal S, Hoffmann K, editors.

Ultrasound in dermatology. Berlin, Heidelberg, New York, London, Paris, Tokyo, Hong Kong, Barcelona, Budapest: Springer; 1992. p. 41-83.
2. Veiro JA, Cummings PG. Imaging of skin epidermis from various origins using confocal laser scanning microscopy. Dermatology 1994;189:16-22.
3. Song HK, Wehrli FW, Ma J. In vivo MR microscopy of the human skin. Magn Reson Med 1997;37:185-91.
4. Huang D, Swanson EA, Lin CP, Shuman JS, Stinson WG, Chang W, et al. Optical coherence tomography. Science 1991;254:1178-81.
5. Schmitt JM, Knüttel A, Bonner RF. Measurement of optical properties of biological tissues by low-coherence reflectometry. Appl Opt 1993;32:6032-42.
6. Hee MR, Izatt JA, Swanson EA, Huang D, Shuman JS, Lin CP, et al. Optical coherence tomography of the human retina. Arch Ophthalmol 1995;113:325-32.
7. Hee MR, Puliafito CA, Wong C, Reichel E, Duker JS, Shuman JS, et al. Optical coherence tomography of central serous chorioretinopathy. Am J Ophthalmol 1995;120:65-74.
8. Izatt JA, Hee MR, Swanson EA, Lin CP, Huang D, Shuman JS, et al. Micrometer-scale resolution imaging of the anterior eye in vivo with optical coherence tomography. Arch Ophthalmol 1994;112:1584-9.
9. Fujimoto JG, Brezinski ME, Teamey GJ, Boppart SA, Bouma B, Hee MR, et al. Optical biopsy and imaging using optical coherence tomography. Nat Med 1995;1:970-2.
10. Pan Y, Engelhardt R, Rosperich J, Hüttmann G, Birngruber R. Measurement of optical-interaction-coefficient of intralipid in visible and NIR range. In: Jacques SL, editor. Laser-tissue interaction. Proc Soc Photo-Opt Instrum Eng 2134A. 1994. p. 354-63.
11. Pan Y, Birngruber R, Rosperich J, Engelhardt R. Low-coherence optical tomography in turbid tissue: theoretical analysis. Appl Opt 1995;34:6564-74.
12. Pan Y, Arlt S, Birngruber R, Engelhardt R. Optical coherence tomography in turbid tissue: theoretical analysis and experimental results. In: Foth HJ, Marchesini R, editors. Optical and imaging techniques for biomonitoring. Proc Soc Photo-Opt Instrum Eng 2628. 1995. p. 239-48.
13. Pan Y, Birngruber R, Engelhardt R. Contrast limits of coherence-gated imaging in scattering media. Appl Opt 1997;36:2979-83.
14. Lankenau E, Koch P, Engelhardt R. An imaging system for low coherence tomography. In: Payne SA, Pollock CR, editors. Trends in optics and photonics, volume on advances in optical imaging and photon migration. Washington (DC): Optical Society of America; 1996. p. 247-9.
15. Pan Y, Lankenau E, Welzel J, Birngruber R, Engelhardt R. Optical coherence gated imaging of biological tissues. IEEE J Selected Top Quantum Electronics Lasers Med Biol 1996;2:1029-34.
16. Schmitt JM, Yadlowsky MJ, Bonner RF. Subsurface imaging of living skin with optical coherence microscopy. Dermatology 1995;191:93-8.
17. Tearney GJ, Brezinski ME, Southern JF, Bouma BE, Hee MR, Fujimoto JG. Determination of the refractive index of highly scattering human tissue by optical coherence tomography. Opt Lett 1995;20:2258-61.